Sustainable Manufacturing of Metal Additive Powders from Machining Scrap

Karan A. Baramate[1]*, Franck Lacan[1], Michael Ryan[1], Soumya Gangopadhyay[2], and Debajyoti Bhaduri[1]

[1] High-Value Manufacturing Research Group, School of Engineering, Cardiff University, Queen's Buildings, Cardiff, CF24 3AA, UK
[2] Department of Mechanical Engineering, Indian Institute of Technology Bhilai, Durg, Chhattisgarh, 491001 India
BaramateKA1@cardiff.ac.uk

Abstract. The paper reports a study on the generation of viable metal additive manufacturing (AM) powders from AA5083 aluminium alloy scrap obtained from conventional milling process. This material recycling route involves multi-stage ball milling (BM) of raw chips using a planetary ball miller with varying ball-to-powder ratio (BPR: 10:1 and 15:1), ball diameter (5, 10, and 20 mm), RPM (150, 300, and 500), jar volume (100 and 250 ml) and BM time (30 and 60 mins). The BM powders were characterised in terms of the particle size distribution, morphology, and phase analysis. Single-track melting of the produced BM powder was subsequently carried out using an in-house laser powder bed fusion (LPBF) system by varying energy density (E_d) (15-134 J/mm^3). Quite expectedly, the height and width of the melted tracks increased with the increase in E_d. The study demonstrates that it is possible to produce BM powders that can be utilised for fabricating AM parts, however further research is imperative in order to achieve the desired size, shape and flowability of the BM powders that can be suitable for LPBF process.

Keywords: Sustainable manufacturing, Additive manufacturing, Ball milling

1 Introduction

Today, additive manufacturing (AM) is considered as the new 'workhorse' for near net shape manufacturing, as evident from the Wohlers Report 2022 (powered by the ASTM International analysis on AM and 3D printing worldwide) that shows a 19.5% growth in the AM industry in 2021 [1]. Despite the numerous benefits offered by AM in terms of the manufacturing flexibility, design freedom and complexity of the parts, the technology itself is energy-intensive, especially the laser powder bed fusion (LPBF) and the directed energy deposition (DED) processes. The stringent requirement of the AM powder properties causes the technology to be even more exhaustive in terms of energy consumption and CO_2 footprint generation. This is because commercial AM powders are typically produced via melting and atomisation techniques, such as gas atomisation, water atomisation, plasma atomisation and ultrasonic atomisation. The gas and water

atomisation begin with heating the initial raw billets of feedstock alloy in a furnace. This causes the material to melt, starting from the top of the atomiser. In the atomisation chamber, a pressurised stream of gas or water is strategically directed to break down and solidify the molten droplets from a nozzle, resulting in nearly spherical particles. These powders are subsequently collected at the bottom of the chamber and supplied as feedstock following the particle size distribution based on requirements of different applications [2].

The United Nation's Sustainable Development Goal 12, also known as SDG 12 is dedicated to achieve responsible consumption and production patterns by the year 2030. The objective of this goal is to acknowledge that the consumption and production practices are frequently unsustainable, resulting in degradation, depletion of resources and social inequalities. SDG 12 strives to tackle these challenges by endorsing sustainable approaches in the production and consumption of goods and services [3]. In the context of industrial waste, a circular economy approach focuses on minimising waste, increasing resource efficiency, and promoting material reuse and recycling throughout industrial operations [4,5]. This research aims to directly address the SDG 12 by developing a novel method of recycling machining scrap/swarf/chips to produce valuable AM powders by solid-state crushing them at room temperature, thereby avoiding the energy-intensive melting and atomisation processes.

Recycling of machining scrap via solid-state crushing, especially ball milling (BM), to produce pallets (via consolidation, compaction, and sintering) [6,7] for powder metallurgy (PM) application [8,9] is known for over ~50 years [10]. However, research into the use of BM powders, generated from machining swarf, for AM applications has only been started in the past ~5 years. The vast majority of research in this context focused on single-track melting of BM particles using DED process [11], whereas use of LPBF is rather limited [14, 15]. This is possibly because of the less stringent requirements of powder properties (sphericity, flowability, packing density,…) in DED, in comparison to that needed for the LPBF process. DED can also adopt the flexibility of utilising BM particles via either powder or wire feedstock, or via direct feeding of machining chips [12]. In this recent study [12], it was observed that DED can create dense and repeatable deposits using 304L stainless steel milling swarf directly with and without coolant using a vibrational feeding system. The deposition was carried on chips with and without the presence of a mineral-based coolant to compare the effects. Thus, it was further validated that the microstructure and mechanical properties of the produced parts were identical in both cases with and without coolant [12]. In their research, Dhami et al. [13] demonstrated generation of consistent and nearly spherical AISI 52100 steel powder particles suitable for AM processes. Although the methodology employed in this research differs significantly from the BM technique, they conducted surface grinding using selected materials and specific speeds. Subsequently, the collected powders underwent analysis for single-track melting within a custom-designed powder-based DED system. The results were then compared with single tracks generated using commercial powders, demonstrating a remarkable similarity [13].

In a different study, multistage ball milling of 304 L stainless steel chips is reported to produce powders for AM [11]. The obtained particle size ranged between 38-150 µm. Deposition of single tracks using laser engineered net shaping (LENS) process,

with a layer thickness of 150, was subsequently carried out. Regarding the use of BM powders in LPBF process, Dhiman et al. [14] utilised a multistage BM of Ti6Al4V swarf and performed single-track melting on a direct metal laser sintering (DMLS) machine. Effective melting of powder was noticed at a laser scanning speed of 1000 mm/s and 350 W power. A further observation was, the dominant effect of using different ball sizes and milling time where ~60% of nearly spherical particles were within the range of 53-150 µm and were obtained when using Ø 6.25 mm diameter balls for 18 hours, following rough BM using Ø 25 mm and Ø 12.5 mm balls for 6 and 12 hours respectively. Additionally, to evaluate the energy consumption of the BM process, a life cycle analysis was conducted in comparison to the gas atomisation process [14].

There is limited evidence on the fabrication of complete AM parts using BM powders [15]. Pfefferkorn et al. [15] compared the characteristics of stainless-steel parts fabricated via DED using both mechanically generated (ball milled) powders and commercially supplied powder. They found similar surface texture, microstructure within both part samples with diverse feedstocks. Nonetheless, significant changes in hardness and tensile strength were observed [15].

Razumov et al. [16] investigated recycling of chips using the same solid-state crushing principle. An attritor BM to grind machining chips of high-alloyed heat-resistant steel Fe-11Cr-1.5Ni-0.2V-0.4Mo-0.1C was used. However, a secondary plasma spheroidisation step was undertaken to achieve spherical particles suitable for both DED and LPBF processes. Printing of cylindrical bulk samples via LPBF and deposition of plates by DED was carried out. Further, the samples were characterised for microstructure observation and mechanical properties (tensile testing). These specimens manufactured using both LPBF and DED exhibited elevated strength levels but with limited plasticity.

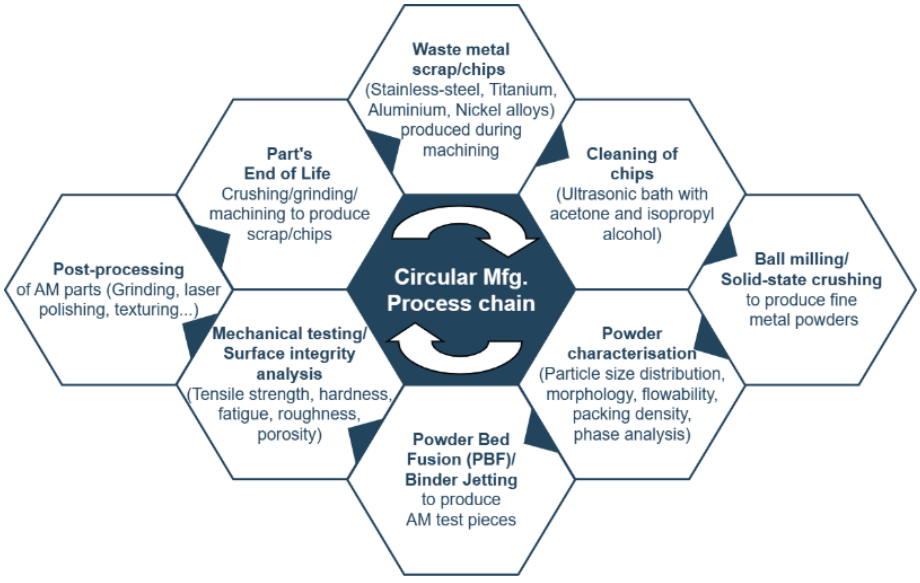

Fig. 1. Step-by-step schematic of circular manufacturing process chain of AM parts.

Despite the sporadic attempt undertaken on the use of BM chip powders to produce AM parts, an in-depth study on the full-scale fabrication of AM components from the recycled scrap, including assessment of their mechanical/thermal/chemical properties, is extremely limited. This research aims at building a novel circular manufacturing process chain to fabricate high value AM parts from production scrap using a cost effective and energy efficient route (see Fig. 1). Dramatic reduction in the CO_2 footprint of the AM powder generation method is targeted via solid-state crushing of machining scrap at room temperature. This is followed by powder characterisation steps and subsequent single-track melting of the produced BM particles on an in-house LPBF system.

2 Materials and methods

2.1 Preparation of the AA5083-H111 machining chips

Chips of AA5083-H111 aluminium alloy, measuring ~1-3 mm in length, were obtained from conventional CNC milling machining. A visual representation of the chips as shown in Fig. 2 (a). The milling operation utilized a 4-tooth carbide end mill cutter with a Ø 16 mm diameter, operating at a cutting speed of 85 meters per minute, a feed rate of 0.24 mm per revolution, and an axial depth of cut of 0.5 mm. In order to eliminate contaminants that arose during the machining process, the chips were subjected to a cleaning procedure involving immersion in an ultrasonic bath using a beaker filled with acetone and subsequently isopropyl alcohol, each for a duration of 15 minutes. Finally, the chips were heat treated by keeping it in an oven for drying at 100°C for 1 hour.

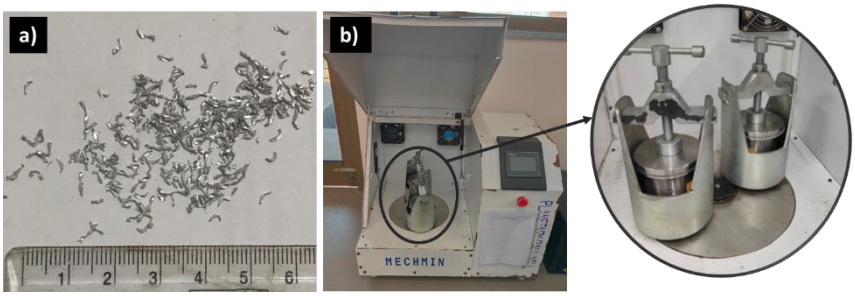

Fig. 2. a) AA5083-H111 chips, b) Planetary BM machine (with enlarged view of its interior).

2.2 Ball milling

After the cleaning process the chips were ball milled to produce powder in a dual station planetary ball mill manufactured by MECHMIN, Ltd., India (Fig. 2 (b). The ball milling was performed at room temperature and in a dry atmosphere. Based on the literature [11] initially different multi-stage BM trials were performed by varying BPR (10:1, 15:1, 20:1 and 30:1), BM speed (150, 300 and 500 RPM), BM time (30, 60 and 90 mins), and jar volume (100 and 250 ml), considering the empty space required for balls' motion inside the jar, with respect to the ball diameter. After visual inspection of the powder particles in terms of their shape and size, two sets with three stages in each set

(see Table 1) were developed to perform the mainstream BM operation, for 60 min (Stage 1 and 3), and 30 min (Stage 2). To prevent the milling media from overheating, a cycle of 15 min BM ON and 10 mins BM OFF (time interval) was implemented. Nearly, 1/3rd volume of jar was kept empty. Therefore, BPR (weight ratio) of 15:1 was appropriately seen feasible for Stage 1, as 20 mm ball requires more volume, and for next two stages with 10 mm and 5mm balls 10:1 BPR was kept constant in both sets.

Table 1. Selected BM parameters in the mainstream trials.

Sets and Stages		BPR	Ball dia. (mm)	Jar volume (ml)	BM Speed (RPM)	BM time (min)
Set 1	Stage 1	15:1	20	250	300	60
	Stage 2	10:1	10	250	300	30
	Stage 3	10:1	5	100	150	60
Set 2	Stage 1	15:1	20	250	300	60
	Stage 2	10:1	10	250	500	30
	Stage 3	10:1	5	100	150	60

Milling balls of hardened stainless steel of 20 (Ø 20), 10 (Ø 10), and 5 mm (Ø 5) diameter were used. Again, considering the proportion of balls and the grinding material, two distinct cylindrical jars made of stainless steel with 250 and 100 ml volume were used in the BM run as shown in Table 1. On a dual station planetary ball mill, 15 off 20 mm, and 50 off 10 mm balls were loaded in each of the 250 ml jars, and 250 off 5 mm balls were used in each 100 ml jar. Rotational speed (BM speed) of 300 RPM and 150 RPM were employed for the 20 and 5 mm balls, respectively. One additional trial was performed with the machine's highest possible speed, i.e., 500 RPM, when using 10 mm balls. (Set 2-Stage 2).

2.3 Powder characterisation methods

For the determination of particle size distribution, mechanical sieving was employed with three sets of sieve sizes: 63 µm, 150 µm and 180 µm. After each stage, the BM particles were sieved to <180 µm and were used for the successive stages. The analysis of powder morphology was conducted using a Carl Zeiss FEG scanning electron microscope (SEM). Phase identification of the raw swarf and powder particles was carried out using a Bruker D8 Advance X-ray diffractometer (XRD) equipped with a Cu-Kα target, employing a 0.03° step size, a scan speed of 0.5 seconds per step, and operating at 40 kV voltage and 30 mA current. The scanning covered a 2θ range spanning from 20° to 90°. The single tracks were analysed using Sensofar SMART 3D profilometer to measure the height and width at three different intervals of the track.

2.4 Single track melting on LPBF system

The powders generated from the Set 2-Stage 3 BM process and sieved below 180 µm were used for single-track melting experiments on a Renishaw's AM250 LPBF system. The process parameters were chosen based on a previous work on LPBF of AA5083-

H111 pre-alloyed powder [17]. Six individual single tracks were generated on a build plate made of the same material using 200 W laser power (LP), 0.18 mm layer thickness, and 0.13 mm hatch spacing. As the system operates using a pulsed laser source, the laser exposure time and relatively scan speed (SS) were varied to achieve six different levels of energy density (E_d) while keeping the point distance constant at 80 µm, see Table 2.

Table 2. LPBF Process parameters used for single track melting trials.

Tracks	Point Dist. (µm)	Exposure time (µs)	Speed (mm/s)	E_d (J/mm^3)
T1	80	125	567	15
T2	80	250	301	28
T3	80	500	155	55
T4	80	750	104	82
T5	80	1000	79	108
T6	80	1230	64	134

A new reduced build volume (RBV) fixture was designed and fabricated in-house to be used on the LPBF machine and to accommodate limited powder quantity produced from the BM process, see Fig. 3 (a, b). While laying the pre-placed powders (sieved to <180 µm) on the built plate, shown in Fig. 3 (c), achieving a layer thickness of 180 µm on the machine was found to be difficult due to the non-spherical morphology of the powder particles. The position of the wiper/recoater was required to be adjusted in order to achieve the desired layer thickness.

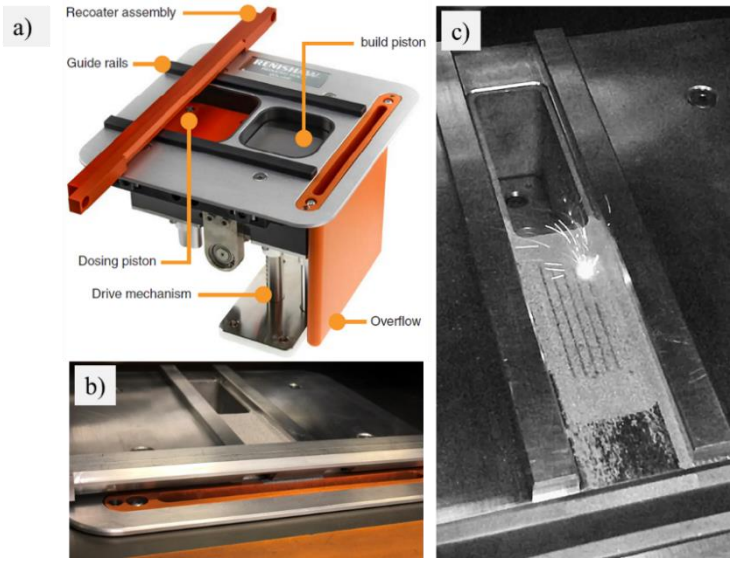

Fig. 3. Design and fabrication of the RBV fixture for the in-house LPBF system: a) Renishaw's existing RBV kit (build plate 80 mm × 80 mm), b) Newly fabricated RBV kit (build plate 25 mm × 75 mm), c) Image captured during the single-track melting with 180 µm layer thickness.

3 Results and discussion

3.1 Characterisation of AA5083-H111 swarf and BM powders

Particle size distribution and morphology. Considering the total chip to powder ratio used for BM, nearly 18% (by weight) of the BM particles were below 180 µm after Stage 1 in both sets and nearly 30% were below 180 µm after Stage 2 in Set 1, relative to the total weight of the BM chips. In contrast, around 63% of the BM powder particles were below 180 µm after Stage 2 in Set 2 (with 500 RPM). The particle size distribution demonstrates that even approximately 70% of the particles were below 180 µm after Set 2-Stage 3.

The histogram bar chart displayed in Figure 4 presents particle size distribution data obtained using three different sieves (63, 150 and 180 µm). After Set 1 in Stage 1, 58% of powder particles were within 150-180 µm, 38% of particles were within 63-150 µm and 4% below 63 µm. In Set 1-Stage 2, particle size gradually reduced: 55% within 150-180 µm, 40% in between 63 to 150 µm and 5% below 63 µm. Further proceeding to Stage 3 rendered 47% particles within 150-180 µm, 45% within 63-150 µm and 8% below 63 µm. The Set 2-Stage 1 data are comparable with that of Set 1. However, marginal increase in the proportion of the particles within 63-150 µm was observed after Set 2-Stage 2. Following Set 2-Stage 3, the proportion of particles within 63-150 µm was even higher (62%). It is evident that the utilisation of a multi-stage ball milling process was effective in reducing the particle size, which is in agreement with [7].

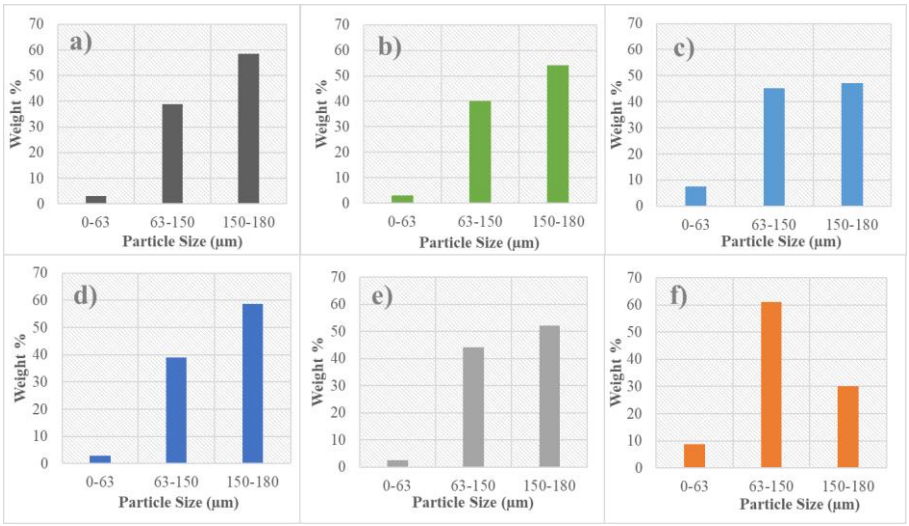

Fig. 4. Particle size distribution obtained via sieving, a) Set 1-Stage 1, b) Set 1-Stage 2, c) Set 1-Stage 3, d) Set 2-Stage 1, e) Set 2-Stage 2, f) Set 2-Stage 3.

Figure 5 shows representative SEM micrographs of raw chips and ball milled powders from Set 1-Stage 1. Typical serration marks are observed on the top surface of the

chips due to welding of the chip segments (Fig. 5 (a)). The BM particles obtained after Set 1-Stage 1 are shown in Fig. 5 (b). Flattening of the particles was noticed due to the high impact force from the 20 mm stainless steel balls on the ductile Al chips/particles that might have resulted in the irregular shape of the particles. Signs of plastic deformation on magnified particles are evident in Fig. 5 (c). In addition, some regions exhibit cleaved fractures, potentially due to the strain hardening effect during BM, resulting from the presence of ~4-4.9% Mg in the alloy.

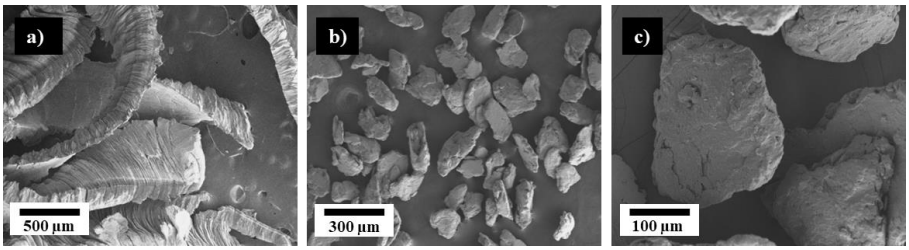

Fig. 5. SEM images: a) Raw AA5083-H111 swarf b), c) BM powders from Set 1-Stage 1

Phase analysis: X-ray diffraction. The XRD analysis of both aluminum chips and ball-milled (BM) powders showed characteristic peaks corresponding to aluminum (Al) and aluminum oxide (Al_2O_3) at their standard 2θ positions 38° and 45°, respectively. However, oxygen content was found on the chips as well as on the particles generated after 1 hour of ball milling at a BPR of 15:1. As BM was conducted under atmospheric conditions, oxidation of the particles might have occurred. It is yet to be realised whether the formation of Al_2O_3 on the particles would provide any benefit in terms of chemical stability/inertness.

3.2 Single track melting on LPBF system

Figure 6 shows the six different tracks melted on the aluminium built plate when using six different laser process parameters. The exposure time with respect to the scan speed (SS) was varied to explore the effects of energy density within the six individual tracks. Thus, in effect, the tracks were deposited with a range of energy density, spanning from lower E_d (T1-15 J/mm^3) to higher E_d (T6-134 J/mm^3).

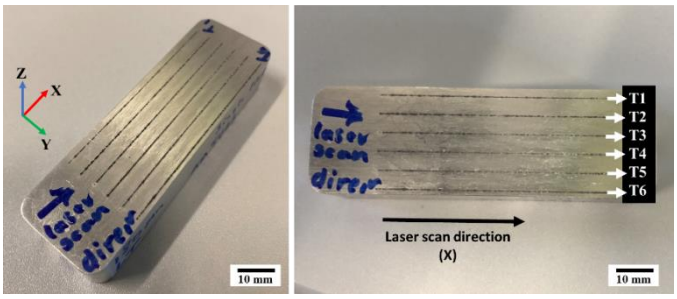

Fig. 6. Images of melted single tracks on the build plate.

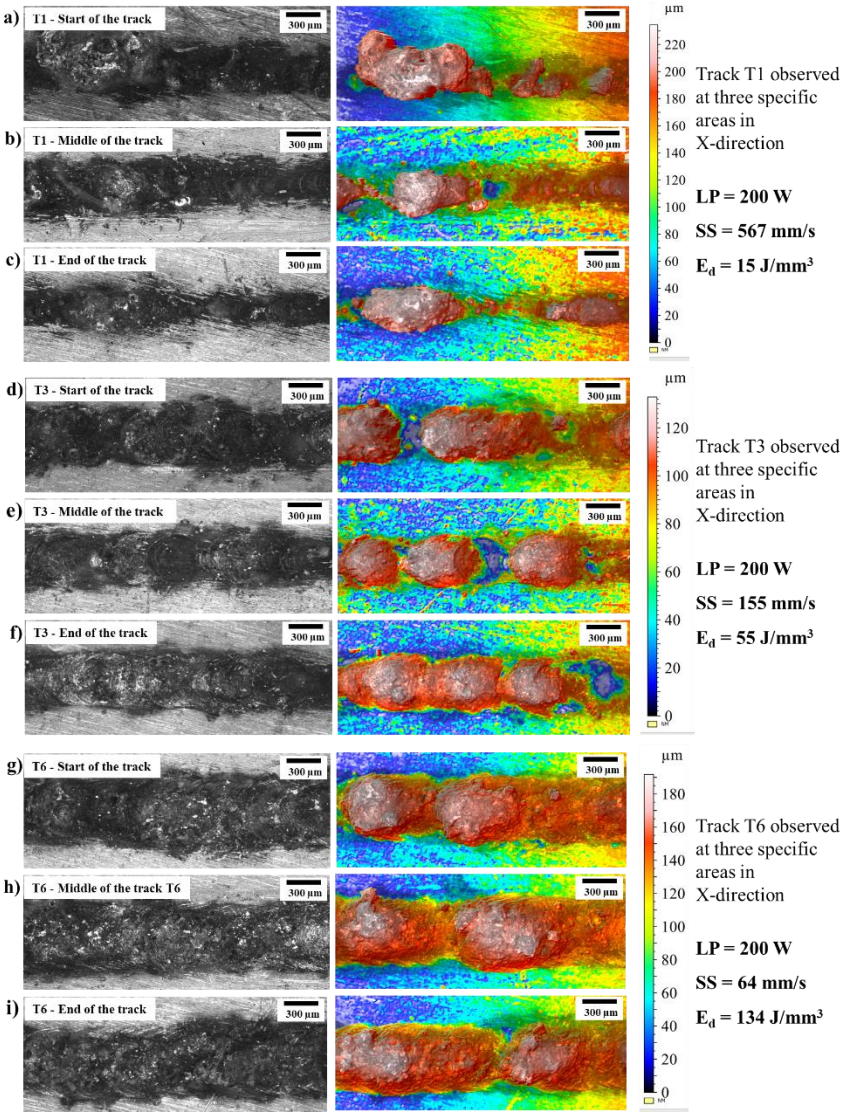

Fig. 7. 3D images and the corresponding height maps of melted single tracks for T1 a) start, b) middle and c) end of the track; for T3 d) start, e) middle and f) end of the track; for T6 g) start, h) middle and i) end of the track.

The 3D images of three single tracks (T1, T3 and T6) and their corresponding height maps are shown in Fig. 7. It clearly indicates that tracks T1 and T3 did not undergo continuous melting as compared to track T6, primarily because the laser did not provide the sufficient exposure time for T1 and T3, thus the energy density was not sufficient enough to fully melt the particles. In contrast, nearly consistent/uniform melting can be

seen in T6 with an exposure time of 1230 µs and scan speed of 64 mm/s, that rendered an energy density of 134 J/mm^3.

The measured average height and width of all the tracks are presented in Fig. 8 (a) and (b) respectively. Tracks T1 and T2 have wider range of height and width values as compared to the others, because of the non-uniform melting at lower energy densities, whereas T3-T6 tracks showed narrower ranges of track height and width. This is also corroborated from Fig. 7 that exhibits a consistent melting pattern on track T6. The average height of T6 falls within a range of 80 to 140 µm, spanning from 25% to 75% of the total range. Additionally, the average width of the track, within the same 25% to 75% range, measures between 325 to 375 µm. This analysis highlights the significant impact of the laser energy density on the melting process.

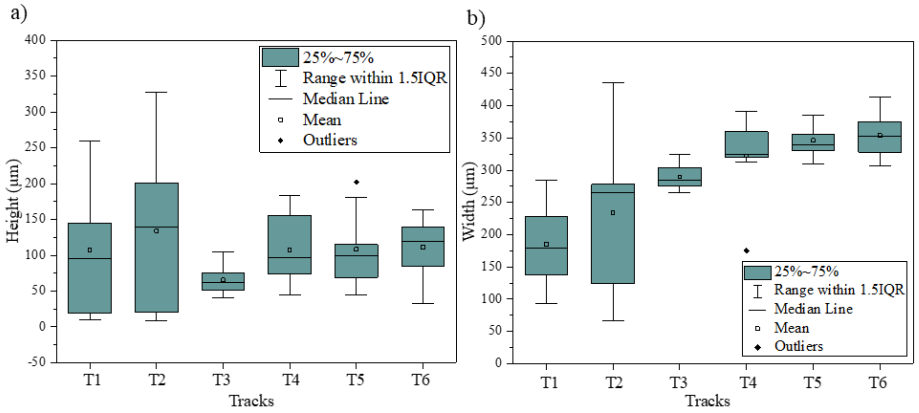

Fig. 8. a) Average data of height acquired and, b) Average data of width acquired by each tracks after single track melting (tracks T1 to T6).

4 Conclusions

- This research explores the viability of a process transformation of machining scrap into AM powders via ball milling, to make them suitable especially for laser powder bed fusion (LPBF) process. The results highlight the importance of optimising different ball milling parameters, including ball-to-powder ratio (BPR), ball milling time, BM speed, ball diameter and material to attain powders with the intended particle size and shape.
- Following a multistage ball milling process, it was observed that the powder particles became nearly spherical, and most particles were below 150 µm. The obtained powders from Set 2-Stage 3 were tested for single track melting using an in-house LPBF machine.
- The results from the analysis of single tracks (using 3D-profilometer) showed that tracks T1 and T3 had significant variations in the degree of melting as well as in their heights and widths throughout the track length. In contrast, track T6 revealed greater uniformity of melting, as evident from the box chart

showing that the average height range of 25-75% data falling between 80 to 140 µm, and the width range of 25-75% data lying within 325 to 375 µm.

- Despite the initial success of this pilot study greater particle sphericity suitable for LPBF process is yet to be achieved. The single-track melting experiments demonstrated the feasibility of utilising BM powders after process development.
- The next phase of the research will involve fabricating AA5083 AM test pieces using the BM powders on the in-house LPBF system. Furthermore, these bulk samples will be tested for microstructure characterisation and mechanical testing (tensile testing, fatigue, hardness…) and will be compared with the parts produced using commercial powders.

5 Acknowledgments

The research is supported by the Government of Maharashtra's (India) PhD studentship award (Rajarshi Shahu Maharaj Foreign Scholarship) and the Net Zero Innovative Institute's (NZII) Seedcorn fund received from Cardiff University.

References

1. Wohlers Report 2022 Finds Strong Industry-Wide Growth, https://wohlersassociates.com/press-releases/wohlers-report-2022-finds-strong-industry-wide-growth/, accessed on 2023/09/01.
2. Dawes, J., Bowerman, R., Trepleton, R.: Introduction to the additive manufacturing powder metallurgy supply chain. Johnson Matthey Technology Review 2015, Vol. 59, pp. 243–256 (2015).
3. Goal 12, Department of Economic and Social Affairs - Sustainable Development: https://sdgs.un.org/goals/goal12, accessed on 2023/07/24.
4. Ellen MacArthur Foundation, Growth within: A circular economy vision for a competitive Europe, https://emf.thirdlight.com/link/8izw1qhml4ga-404tsz/@/preview/1?o, accessed on 13/08/2023.
5. Kirchherr, J., Yang, N. N., Schulze-Spüntrup, F., Heerink M. J., Hartley, K.: Conceptualizing the Circular Economy (Revisited): An Analysis of 221 Definitions, Resources, Conservation and Recycling 2023, vol. 194, 107001. Denmark (2023).
6. Teja, P. J., Shial, S. R., Chaira, D., Masanta, M.: Development and characterization of Ti-TiC composites by powder metallurgy route using recycled machined Ti chips. Materials Today: Proceedings (26), pp. 3292-3296 (2020).
7. Shial, S. R., Masanta, M., Chaira, D. Recycling of waste Ti machining chips by planetary milling: Generation of Ti powder and development of in situ TiC reinforced Ti-TiC composite powder mixture. Powder Technology, Vol. 329, pp. 232-240 (2018).
8. Rojas-Díaz, L. M., Verano-Jiménez, L. E., Muñoz-García, E., Esguerra-Arce, J., Esguerra-Arce, A.: Production and characterization of aluminum powder derived from mechanical saw chips and its processing through powder metallurgy. Powder Technology, vol. 360, pp. 301–311 (2019).
9. Pulido-Suárez, P. A., Uñate-González, K. S., Tirado-González, J. G., Esguerra-Arce, A., Esguerra-Arce, J.: The evolution of the microstructure and properties of ageable Al-Si-Zn-

Mg alloy during the recycling of milling chips through powder metallurgy. Journal of Materials Research and Technology. Vol. 9, pp. 11769-11777 (2020).
10. Lawley, A. Preparation of metal powders. Annual Review Material Science, vol. 8, pp no. 49-71 (1978).
11. Fullenwider, B., Kiani, P., Schoenung, J. M., Ma, K: Two-stage ball milling of recycled machining chips to create an alternative feedstock powder for metal additive manufacturing. Powder Technology, vol. 342, pp. 562-571 (2019).
12. Murray, J. W., Speidel, A., Jackson-Crisp, A., Smith, P.H., Constantin, H., Clare, A.T.: Unprocessed machining chips as a practical feedstock in directed energy deposition. International Journal of Machine Tools and Manufacture, vol. 169, 103803 (2021).
13. Dhami, S. H., Panda, P. R, Vishwanathan, K.: Production of powders for metal additive manufacturing applications using surface grinding. Manufacturing Letters, vol. 32, pp no. 54-58 (2022).
14. Dhiman, S., Joshi, R. S., Singh, S., Gill, S. S., Singh, H., Kumar, R., Kumar, V.: Recycling of Ti6Al4V machining swarf into additive manufacturing feedstock powder to realise sustainable recycling goals. Journal of Cleaner Production, vol. 348, 131342 (2022).
15. Jackson, M. A., Morrow, J.D., Thoma, D.J., Pfefferkorn, F.E.: A comparison of 316 L stainless steel parts manufactured by directed energy deposition using gas-atomized and mechanically-generated feedstock. CIRP Annals Manufacturing Technology, vol. 69, pp. 165-168 (2020).
16. Razumov, N. G., Masaylo, D.V., Silin, A.O., Borisov, E.V., Ozerskoy, N.E., Goncharov, I. S., Popovich, A. A.: Investigation of additive manufacturing from the heat-resistant steel powder produced by recycling of the machining chips. Journal of Manufacturing Processes, vol. 64, pp. 1070-1076 (2021).
17. Zhao, L., Hyer, H., Park, S., Pan, H., Bai, Y., Rice K. P., Sohn, Y.: Microstructure and mechanical properties of Zr-modified aluminium alloy 5083 manufactured by laser powder bed fusion. Additive Manufacturing, vol. 28, pp. 485-496 (2019).